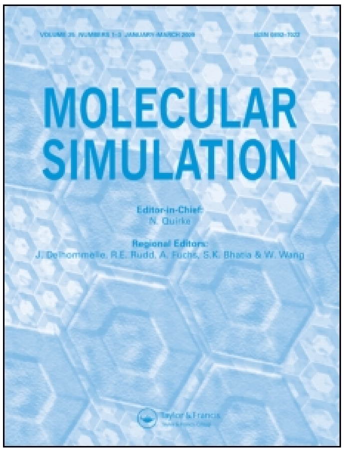

Molecular Simulation
Publication details, including instructions for authors and subscription information:
http://www.informaworld.com/smpp/title~content=t713644482

Multi-Representation Techniques for Multi-Scale Simulation: Reactive Microflows in a Catalytic Converter

S. Succi[a]; M. Adamo[a]; G. Bella[b]; M. Bernaschi[a]
[a] Istituto Applicazioni Calcolo, Rome, Italy [b] Mechanical Engineering Dept., University of "Tor Vergata", Rome, Italy

To cite this Article Succi, S. , Adamo, M. , Bella, G. and Bernaschi, M.(2000) 'Multi-Representation Techniques for Multi-Scale Simulation: Reactive Microflows in a Catalytic Converter', Molecular Simulation, 25: 1, 13 — 26

To link to this Article: DOI: 10.1080/08927020008044109

URL: http://dx.doi.org/10.1080/08927020008044109

Molecular Simulation, 2000, Vol. 25, pp. 13-26
Reprints available directly from the publisher
Photocopying permitted by license only

MULTI-REPRESENTATION TECHNIQUES FOR MULTI-SCALE SIMULATION: REACTIVE MICROFLOWS IN A CATALYTIC CONVERTER

S. SUCCI[a,*], M. ADAMO[a], G. BELLA[b] and M. BERNASCHI[a]

[a]*Istituto Applicazioni Calcolo, Rome, Italy;*
[b]*Mechanical Engineering Dept., University of "Tor Vergata", Rome, Italy*

(Received April 1999; accepted May 1999)

We describe the basic ideas behind a multi-representation (floating-point and integer) algorithm for the numerical simulation of reactive flows with heat transfer. In particular, we provide some details on the interface connecting the integerized to the floating-point components. An application to catalytic conversion is briefly discussed.

Keywords: Multi-representation techniques; multi-scale simulation; reactive microflows; catalytic converter

INTRODUCTION

Most complex phenomena in science and engineering involve the mutual interaction of various physical mechanisms, often proceeding at vastly disparate scales in space an time [1]. The dynamics of reactive flows is a typical example of such phenomena. Besides geometry, the complexity of reactive flow dynamics can be grossly parametrized by means of two dimensionless quantities: the Reynolds number $\mathrm{Re} = UL/\nu$ and the Damkohler number $\mathrm{Da} = \tau_h/\tau_c$, where, U and L denote a macroscopic speed and length of the flow, respectively, whereas τ_c and τ_h represent typical timescales of chemical and hydrodynamic phenomena. High Reynolds numbers spell turbulence, namely loss of coherence in both

---

[*] Corresponding author.

space and time. Low Damkohler numbers imply that chemistry is much slower than hydrodynamics, so that chemical reactions take place at mechanical equilibrium (*perfectly stirred reactor regime*). High Damkohler numbers identify the opposite regime where chemistry is much faster than hydrodynamics, so that chemical reactions are always in equilibrium and take place in tiny regions (thin flames, reaction sheets) of the flow. The interaction between turbulence and fast chemistry is one of the leading edges of computational physics.

Most of the numerical problems relate to the wide spectrum of chemical time-scales, which ultimately result from the non analytic dependence on the temperature of the Arrhenius factor $e^{-T/T^{\mathrm{att}}}$, T^{att} being the activation temperature of a given reaction. This wide spectrum of scales makes the problem "numerically stiff", in the sense that tracking explicitly the shortest scales may often become impractical, not to say prohibitive, for numerical solvers. In addition, owing to the aforementioned non-analytic temperature dependence, sensitivity to small temperature fluctuations may easily induce numerical drifts due to round-off errors intrinsic to the floating-point representation of real number. Round-off errors and related cumulative error pile-up must be constantly watched out in reactive flow simulations. This is why reactive flow simulations are almost a byword for double-precision applications.

In an ideal world, one would like to simulate these problems with *round-off free*, fast explicit methods. *Round-off freedom* is precisely the highlight of a new computational paradigm known as *Digital Physics* [2].

Digital Physics (DP) is based on the idea of representing physical observables by means of *integer*, rather than floating-point, numbers. These integer variables are most sensibly interpreted as *computational molecules* representing a (large) collection of true physical molecules. The integer representation automatically ensures *exact* computation within the allowed range of variability. Historically, DP developed as a spin-off of a more radical approach known as Lattice Gas Cellular Automata (LGCA) [3, 4], in which the physical variables are just binary numbers, *i.e.*, they can only take values 0 or 1, coding for the absence/presence of a computational degree of freedom at a given space-time location. Physical observables, such as fluid density, speed, temperature are then obtained by statistical averaging over large ensembles of 'microscopic' boolean degrees of freedom. The LGCA approach ensures not only round-off freedom but also automatic protection from underflow/overflow errors, because all stages of the computation can be organized in such a way as to preserve the boolean nature of the computational variables (Automata). In revenge, they involve a relatively high amount of statistical noise (like all particle methods) and, what's more, in the process of formulating the physical laws in a purely boolean language, they introduce spurious physical effects known as *anomalies* (common to most lattice field theories). The wish to fix anomalies prompted out a new class of floating-point techniques, known as Lattice Boltzmann method [5]. DP was also generated in response to the same need, with the important characterization of retaining the *integer* (not boolean, though) nature of the computational degrees of freedom.

DP has proved fairly successful for the simulation of complex hydrodynamic flows [6] and has also recently been extended to the case of simple flows with chemical reactions [7, 8]. In this paper we describe the set-up of a hybrid computational scheme combining the Digital Physics approach with a more traditional floating-point (FP) approach. The paper is organized as follows. In Sections 2 and 3 we present the basic equations of reactive flows and the computational method respectively. In Section 4 we discuss the computer program layout, including the handshaking portions between the DP and FP (floating-point) components. Section 5 deals with an application to the problem of catalytic conversion.

REACTIVE FLOW EQUATIONS

We shall deal with a *thermal flow* with *chemical reactions*.

The basic equation of motions are

Fluid Flow:

$$\partial_t \rho + \operatorname{div} \rho \mathbf{u} = 0 \tag{1}$$

$$\partial_t \rho \mathbf{u} + \operatorname{div} \rho \mathbf{u}\mathbf{u} = -\nabla P + \operatorname{div} \mu \nabla \mathbf{u} \tag{2}$$

Temperature dynamics

$$\partial_t \rho T + \operatorname{div} \rho \mathbf{u} T = -\nabla P \bullet \nabla u + \operatorname{div} \mu \nabla \mathbf{u} + \dot{Q} \tag{3}$$

where ρ is the flow density, $\mathbf{u}$ the flow speed, $P = \rho T$ the pressure, T the temperature and μ the dynamic viscosity.

The heat source term reads

$$\dot{Q} = \sum_{r=1}^{R} \dot{\omega}_r Q_r \tag{4}$$

where the sum extends over the complete set of R reactions, each reaction proceeding at a rate $\dot{\omega}_r$, and releasing/absorbing Q_r heat units.

Multispecies transport with chemical reactions

$$\partial_t \rho_s + \operatorname{div} \rho_s \mathbf{u_s} = \operatorname{div} D_s \nabla(\rho_s/\rho) + \dot{\omega}_s \tag{5}$$

where s denotes the generic species.

The species couple *via* the chemical source term

$$\dot{\omega}_s = W_s \sum_r (b_{rs} - a_{rs}) \dot{\omega}_r \tag{6}$$

where a_{rs}, b_{rs} are the forward/backward stoichiometric coefficients of the s species in reaction r, and W_s is the molar weight of species s.

COMPUTATIONAL METHOD

The flow-temperature fields are solved by Arbitrary Lagrangian Eulerian finite volume techniques [9]. Since these methods have become a standard in numerical combustion, we do not need to delve into further details.

The multispecies transport and chemical reactions are handled instead with a Digital Physics approach, namely an integerized variant of the Lax-Wendroff scheme [8]. Within this approach each species is associated with n_{si} is the *occupation number* of species s along the i-th direction $\mathbf{c}_i$ defined in the lattice.

The lattice connectivity vectors are typically interpreted as the discrete speeds of fictitious computational molecules which are bound to move only along the lattice links. With this interpretation, the species densities and current densities are simply obtained as weighted sums over all possible discrete speeds

$$\rho_s = m_s \sum_i n_{si}, \quad \rho_s \mathbf{u_s} = m_s \sum_i n_{si} \mathbf{c}_i, \tag{7}$$

where m_s is the mass of species s.

The digital transport scheme is organized in such a way to involve only the overall species densities, summed all over discrete speeds $n_s = \sum_i n_{si}$.

With these preparations, the transport operator reads as follows (in units $\Delta t = 1$):

$$n_s(\mathbf{x}, t) = \sum_j p_j(\mathbf{x} - \mathbf{c}_j, t - 1) n_s(\mathbf{x} - \mathbf{c}_j, t - 1) \tag{8}$$

The index j runs over a neighborhood of $\mathbf{x}$, and the break-up coefficients represent the probability that a particle at $\mathbf{x}_j \equiv \mathbf{x} - \mathbf{c}_j$ moves along link j to contribute at $n_s(\mathbf{x})$ at time t. These break-up probabilities are in charge of the entire directional dependence on the discrete direction i.

The exact expression of these coefficients (in lattice units $c_i = \pm 1$, $i = 1,2$, $\Delta t = 1$) is (one-dimension is assumed for simplicity):

$$p_i(x \pm 1, t-1) = \frac{1 \mp u'}{2} + D_s', \; i = 1,2 \tag{9}$$

$$p_0(x, t-1) = -2D_s' \tag{10}$$

where $u' = (u + \rho^{-1}\partial_x \rho)$ is the effective speed, inclusive of the density gradient component, and $D_s' = D_s(1 - u'^2)/2$ is the effective diffusion, the square u' dependence being dictated by arguments of numerical stability.

The chemical operator reads as follows

$$\dot{\omega}_s \equiv n_s' - n_s = -K_f \prod_s n_s^{f_s} + K_b \prod_s n_s^{b_s} \tag{11}$$

where the backward/forward rates are assumed in the Arrehnius form

$$K_{f,b} = A_{f,b}\, e^{-T^A_{f,b}/T} \tag{12}$$

where $A_{f,b}$ are given constants and $T^A_{f,b}$ is the backward/forward activation temperature of the reaction. The implementation of the chemical operator raises a number of technical challenges, namely

- Noise correlation build-up,
- Dynamic range bounds,
- Numerical stiffness.

Noise correlation pertains to the fact that non-unit stoichiometric coefficients stemming from multi-molecular reactions lead to potential correlation build-up due to non vanishing even-moments of the particle fluctuations: $\langle n_s^2 \rangle - \langle n_s \rangle^2 \geq 0$. This correlation build-up is a potential source of troubles, as it may introduce anomalous many-body fluctuations into the hydrodynamic evolution due to the paucity of computational molecules (typically $1:10^8$).

Dynamic range pertains to the fact that many chemical reactions involve large excursions of the species concentrations; for instance radicals like H, OH may easily ride across 5–6 decades during the induction phase of a chemical reaction. This sets an obvious constraint on the minimal number of bits needed to represent the integer state of a given species. Let R the dynamic range (maximum to minimum value over the entire evolution) spanned by the evolution of a given species, the minimum number $n_{\min}$ of bits required to encompass R with no under/overflows is given by $2^{n}_{\min} > R$. With $n_{\min} = 16$, the value used throughout this paper, we can track $R = 64\,\mathrm{K}$, *i.e.*, between four and five decades.

This is the best *on-site* accuracy we can get, the idea being that competitivity with floating-point accuracy is gained *via* ensemble averaging and, even more so, *via* absence of round-off errors due to the integer representation.

Finally, stiffness is the general problem associated with the fact that, depending on the temperature (non-analytic temperature dependence in the Arrehnius factor), chemical reactions can span a wide spectrum of timescales, ranging from nanoseconds to fractions of seconds [10].

In a recent time, we have devoted a significant effort to overcome each of these problems [7].

Noise-induced many-body correlations are controlled by introducing multiple realizations (*replicas*) of the same species, and letting them evolve independently, only to recombine every now and then to produce a single physical value. The problem of dynamic range is tackled by allowing a separate normalization for each species (*multi-range* normalization). For instance, radicals are normalized between, say, $10^{-10} - 10^{-6}$(mole/cc) while primary species may vary between say $10^{-5} - 10^{-1}$mole/cc. Finally stiffness is handled "head-on", *via explicit time-stepping*. The idea is that the DP dynamics proceeds on such high-resolution grids as compared with traditional Fluid Dynamics methods, that the hydrodynamic time step can be made short enough to track most chemical reactions explicitly. Obviously, this optimistic stance cannot be secured for all possible flow and chemical conditions: especially at high-temperatures, one should be prepared to cater for adaptive fractional timestepping, namely time-step subcycling on selected regions (hot-spots) of the flow where most of the chemical activity takes place.

In fact current estimates place the lower bound threshold for subcycling at about 1 microsecond. This rough estimate is based on the traversal time of a computational cell $\Delta t = \Delta x / c$ where c is the sound speed. Assuming a reacting flow confined in a cube 1 meter in size, with 10^9 grid-points (thousand per side) we obtain $\Delta x = 0.1$ centimeters and $\Delta t \sim 3$ microseconds.

STRUCTURE OF THE COMPUTATIONAL PROGRAM

The simulation of a reactive flow system is to all effects a *multi-physics* problem, as it involves five distinct physical processes:

1. Fluid Flow (F),
2. Heat Flow (H),
3. Species Transport (T),
4. Chemical Reactions (C),
5. Fluid-Wall Interaction (W) (see Eq. (14) below).

The first three processes are decidedly macroscopic in character, whereas an in-depth treatment of heterogeneous catalysis on the wall would surely call for genuinely multi-physics modelling involving the mesoscopic and microscopic level. By mesoscopic level, we mean the diffusion of gaseous molecules in the solid (ceramic) matrix, which is typically addressed by kinetic Monte-Carlo treatment [11]. At a more fundamental level, one should describe the details of catalytic reactions at the atomic scale, a task which requires the use of quantum-chemistry tools, such as density functional theory and related methods [12].

Our present analysis is however confined to a single-level macroscopic representation of all five processes in point. We can't help but noting, that the DP particle-like formalism is well placed to accommodate the aforementioned multi-level computational approach.

Given the fully explicit nature of the computational method, each of these physical processes can be associated with a corresponding evolution operator, $\mathcal{F}$, $\mathcal{H}$, $\mathcal{T}$, $\mathcal{C}$, $\mathcal{W}$, such that the overall evolution of the system can be formally written in Liouvillean form:

$$\partial_t \Psi = \mathcal{L} \Psi \tag{13}$$

where $\Psi = [\rho_1, \ldots, \rho_{N_s}, \mathbf{u}, T]$ is the state vector of the overall system and $\mathcal{L} = \mathcal{F} + \mathcal{T} + \mathcal{W} + \mathcal{C} + \mathcal{H}$ is the Liouville operator. The ordering of this operator sum is not arbitrary and shall be discussed shortly. For now, we notice that since each of these five operators could in principle be represented in DP or FP format, a host of $2^5 = 32$ possible representations opens up. In the present implementation, processes T, C, W are represented in DP mode, whereas F, H are given a floating-point representation. This choice is not necessarily the optimal one, but only responds to the wish of testing the DP representation under possibly the most severe conditions, which is multicomponent reactive transport (where the range issue is likely to be mostly stringent).

The flow diagram of the current implementation is as follows

```
   DP      FP
==================
           H
. . . . . . . . . . . . . . . . . . . .  t
   T <---- F

   W

   C ----> H
. . . . . . . . . . . . . . . . . . . .  t+dt
           F
```

SKETCH 1 Sketch of the DP and FP evolutionary threads.

The FP-DP leftward arrow implies the communication of the velocity field needed to advect the chemical species. The DP to FP rightward arrow implies the communication of the DP computed reaction rates, which are used to compute the heat source term in the temperature equation. This communication is managed by a thin interface of handshaking routines.

Each of these processes is characterized by its own timescale τ_p, $p = F, H, T, C, W$, which may differ considerably from process to process depending on the local thermodynamic conditions. Thus, the time-marching schedule requires some care. To date, the time-step control is gauged around the transport scale τ_T: processes moving faster than τ_T are sub-cycled τ_p/τ_T times, whereas the slower ones are either overresolved, *i.e.*, they proceed with $dt = \tau_T$ anyway, or supra-cycled, namely they execute only every τ_p/τ_T cycles. The latter practice is more aggressive and generally saves CPU time, but runs the risk of loosing time-step control if a 'sleeping' process wakes up abruptly during supra-cycling. A safety factor on the maximum allowed change for any given physical quantity, typically 0.2, is recommended.

NUMERICAL RESULTS: CATALYTIC FLOW

The application in point refers to an exhaust flow in a catalytic converter. The geometry is a rectangular duct with prescribed species inflow at the inlet and open outlet boundary conditions. On the upper and lower reactive walls, the flow speed is forced to vanish, whereas the fluid-wall mass exchange modelled *via* a mass transfer rate equation of the form

$$\frac{dX_s^w}{dt} = K_s(X_s^g - X_s^w) \tag{14}$$

where superscripts g and w refer to gas and wall respectively, and K_s is a geometry (surface-to-volume of the coating layer) dependent effective transfer rate, with the dimension of a frequency $(1/s)$, which scales with the diffusion coefficient D_s.

Here $X_s = n_s/\sum_{s'} n_{s'}$ represents the *molar fraction* of the s-th species. Within each cell of the wall layer the species evolve accordingly to the following chemical reaction pattern [13]

$$2CO + O_2 \rightarrow 2CO_2, \quad (Q = 0.28,\ T_{att} = 12556) \tag{15}$$

$$2C_3H_6 + 9O_2 \rightarrow 6CO_2 + 6H_2O, \quad (Q = 1.9,\ T_{att} = 361) \tag{16}$$

$$2H_2 + O_2 \rightarrow 2H_2O, \quad (Q = 0.24,\ T_{att} = 11161) \tag{17}$$

where the reaction heats Q are given in MJ/mole and the activation temperatures in Kelvin degrees. The corresponding set of *empirical* reaction rates (moles/cm^2/s) is as follows

$$\dot{\omega}_{CO} = \frac{k_1 X_{CO} X_{O_2}}{G} \tag{18}$$

$$\dot{\omega}_{C_3H_6} = \frac{k_2 X_{C_3H_6} X_{O_2}}{G} \tag{19}$$

$$\dot{\omega}_{H_2} = \frac{k_1 X_{H_2} X_{O_2}}{G} \tag{20}$$

$$\dot{\omega}_{O_2} = \omega_{CO}/2 + 9\omega_{C_3H_6}/2 + \omega_{H_2}/2 \tag{21}$$

where X_s is the molar fraction of species s.

The denominator G is an empirical factor given by

$$G = T\left(1 + h_1 X_{CO} + h_2 X_{C_3H_6}\right)^2 \left(1 + h_3 X_{CO}^2 X_{C_3H_6}^2\right)\left(1 + h_4 X_{NO}^{0.7}\right) \tag{22}$$

The constants k_i, h_i are in the usual Arrehnius form: $k_i = A_i^1 e^{-T_i^{att}/T}$, $h_i = A_i^2 e^{-T_i^{att}/T}$, $i = 1, 3$. Note that $G/T \rightarrow 1$ in the limit of very low concentrations, showing the limiting effect of G on the reactivity at high density regimes. The empirical character of this reaction set reflects the lack of a more fundamental approach along the lines discussed previously.

Chemistry only takes place at the gas/solid interface, which means that the reaction section of the numerical code is confined to a pair of monolayers of computational cells at $y = 0$ and $y = H$. Since we are mainly interested in a proof-of-concept, the DP-FP code has been run on a relatively low resolution 101×11 grid, corresponding to a 10 cm long and 1 cm wide catalytic channel. This shows that we are indeed dealing with a microhydrodynamic flow.

Thermodynamic conditions are as follows: $P = 1.47$ Atm, $T = 600$ K in the bulk and $T_w = 300$ K in the lower and upper walls. The species are continuously fed in at the inlet ($x = 0$) according to a prescribed spatio-temporal schedule $\rho_{s0}(y,t) \equiv \rho_s(x = 0, y; t)$. For the sake of simplicity, numerical tests refer to the case where the inlet conditions are constant in time and all along the vertical coordinate, namely $\rho_s(x, y, t = 0) = \rho_s^0$. The initial values, in grams per centimeter cube, are $\rho_{CO}^0 = 3.01\,10^{-4}$, $\rho_{C_3H_6}^0 = 1.69\,10^{-4}$, $\rho_{O_2}^0 = 5.67\,10^{-2}$, $\rho_{CO_2}^0 = 0$, $\rho_{NO}^0 = 3.33\,10^{-6}$, $\rho_{H_2}^0 = 4.01\,10^{-4}$, $\rho_{H_2O}^0 = 0$, and the inlet speed $U^0 = 1000$ (cm/s). This corresponds to a cell residence time $\tau_h = 0.1$ ms, generally shorter than the typical chemical timescale except in the "light-off" stage of the reaction (see below).

Qualitatively, the physical picture is as follows. Owing to molecular diffusion, species are continuously transported from the bulk to the wall, and so does temperature. In the absence of any chemical activity at the walls, the wall densities would just grow till they come in balance with the bulk values. This behaviour has indeed been observed in the simulations with inert flows. With chemistry on, the picture is obviously richer. Chemistry lays dormant until a sufficient temperature and density build-up is accumulated at the wall. From there on, chemistry rapidly proceeds to consumption of the reacting species and release of the reaction products. This qualitative scenario is indeed reflected by the results shown in Figure 1, which reports the time evolution of the molar concentration (moles/cell) of the *propilene* (C_3H_6), at the location $x = 7$ in the bottom wall $y = 0$.

The DP results (solid line) are compared with the floating-point solver (dashed line). The two sets of data compare satisfactorily, in that, besides showing reasonable quantitative agreement, they exhibit the same sharp decay due to chemical light-off basically at the same time, $t \sim 20$ ms. Of course, some discrepancy in the concentration is also visible in the ramp-up stage. This discrepancy might well be due to minor differences in the

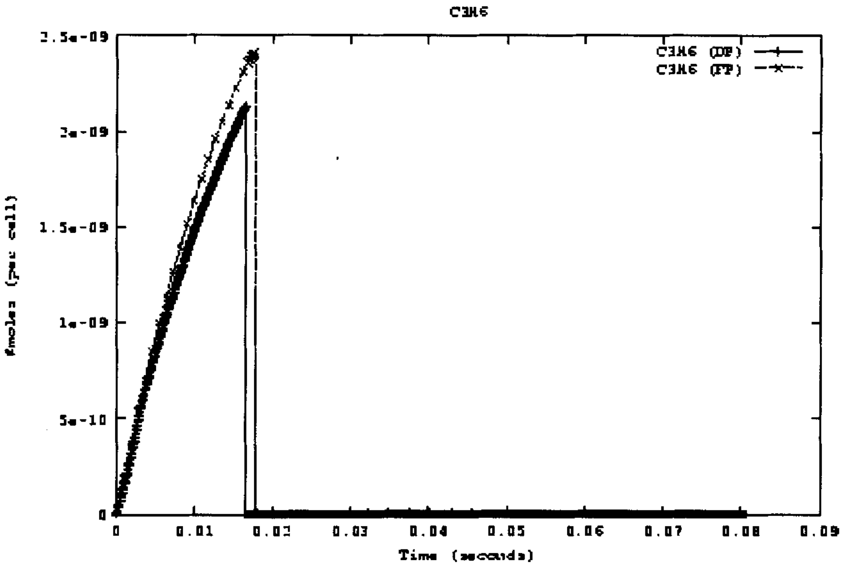

FIGURE 1 C_3H_6 at $x = 7$, $y = 0$ as a function of the time. Digital and floating-point simulation. The species concentration is in moles per computational cell.

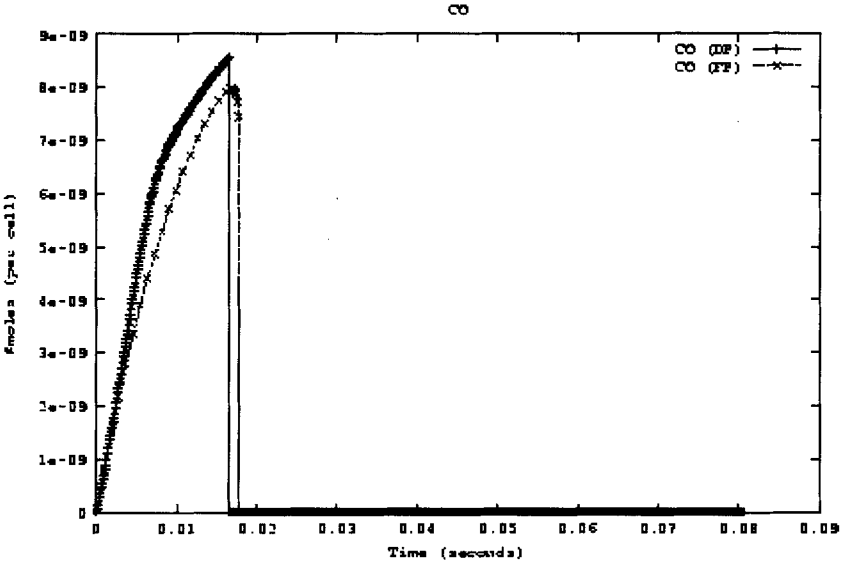

FIGURE 2 CO at $x = 7$, $y = 0$ as a function of time. Digital and floating-point simulation. The species concentration is in moles per computational cell.

floating-point and digital initial data, as well as to the time-stepping procedure which cannot be guaranteed to be exactly the same. In Figure 2 we show the molar concentration of the main reactant, *carbon monoxide* at a near-inlet location on the lower wall ($x = 7, y = 1$).

As expected, the behaviour is essentially the same as for C_3H_6. Similar, but complementary, behaviour is also observed for the products of the reaction.

Finally, we report in Figure 3 the temperature evolution of both the digital and the floating-point simulation.

The temperature evolution is characterized by three distinct stages: (i) Induction, (ii) Light-off, (iii) Saturation.

Phase (i) is characterized by a mild temperature increase due to the transportive bulk-to-wall heat transfer. Once this mild heating brings the wall temperature in the vicinity of the smallest activation temperature ($T^{\text{att}} = 361$ for reaction 2 in our case), and a concomitant wall density build-up takes place, chemistry starts-off abruptly. This is the light-off stage, characterized by a very steep, chemistry-controlled, temperature rise. This is also the stage in which substantial catalytic conversion takes place (see Figs. 1, 2). Eventually, phase (ii) comes to an end due to lack of reactants, and a second transport-controlled mildly rising temperature regime sets in, which eventually takes the system to a steady state. In case

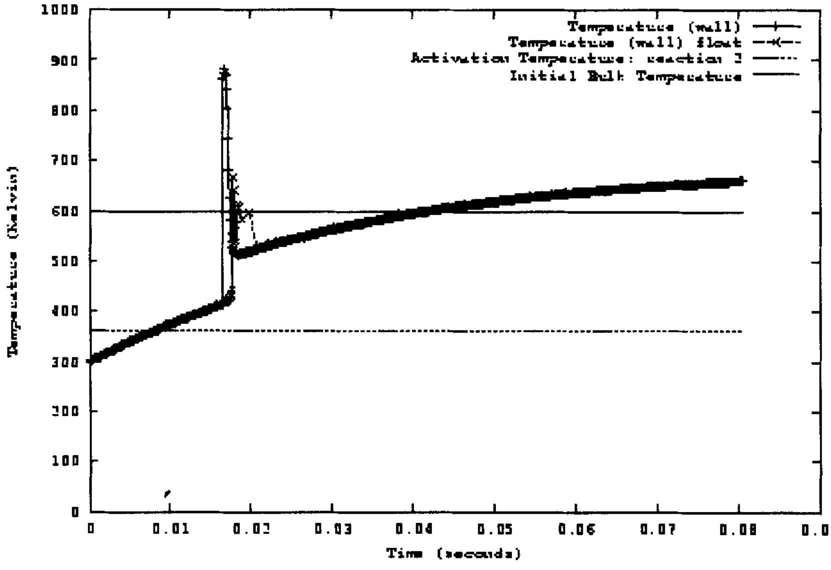

FIGURE 3 Temperature at $x = 7$, $y = 0$ as a function of time.

the light-off phase brings the wall temperature above the bulk one, with a consequent wall-to-bulk inverted heat flow, a fourth temperature-decaying, 'post-light-off' regime is eventually observed. This is indeed the case for the present simulation.

A glance at Figure 3 shows that the FP code has some pain in tracking the sharp light-off and post-light off phases, whereas the DP-FP approach seems to do better (no oscillations). Quantitative agreement between the two versions is lost for a short while, but it is quickly regained within a few milliseconds.

Before concluding, a few words on the computational performance are in order. The code starts with a timestep $\Delta t \sim 9\,\mu\text{s}$, a value that needs to be reduced by a factor ten during the lightoff stage. Since this stage only lasts a few milliseconds, the impact on the overall performance is negligible. Approximately 10^4 steps are required in order to attain the steady state. At about 0.2 CPU seconds/step, corresponding to 100 μs/site/step (on a Sun UltraSparc with a clock rate of 167 MHz), this means roughly a hour per simulation. Since the computing time scales linearly with the size of the grid, large-scale three-dimensional simulations surely require parallel computers.

DISCUSSION

We have presented the main ideas behind the hybrid Digital Physics-Floating-Point approach for thermal reactive flow modeling. Preliminary results pertaining to a two-dimensional flow in a catalytic converter show encouraging agreement with corresponding floating-point methods. They also show that further work is needed to gain a better understanding of the robustness of the integer representation in the various parameter regimes.

As a near-term future application, we plan to study the effects of microturbulence induced by geometrical/structural microirregularities, on the overall catalytic conversion efficiency. On a much longer-term, a truly multi-physics coupling to kinetic Monte-Carlo methods for gas diffusion in the solid matrix and a quantum-chemical treatment of elementary catalytic events, is also in focus.

Acknowledgement

S. S. acknowledges financial support from EXA Corporation during several stays in Boston.

References

[1] Abraham, F., Broughton, J., Bernstein, N. and Kaxiras, E. (1998). *Comp. in Physics*, **12**(6), 538.

[2] Molvig, K., Donis, P., Myczkowski, J. and Vichniac, G. (1992). In: *Discrete Kinetic Theory, Lattice Gas Dynamics and Foundations of Hydrodynamics*, Monaco, R., Ed., World Scientific 1988 and Teixeira, C., *Ph.D. Thesis*, M.I.T.

[3] Frisch, U., Hasslacher, B. and Pomeau, Y. (1986). *Phys. Rev. Lett.*, **56**, 1505.

[4] Doolen, G. D. Ed. (1993). Lattice Gas Methods for PDE's: Theory, Applications and Hardware, Oct., 1990, *Physica D*, **47**.

[5] Benzi, R., Succi, S. and Vergassola, M. (1992). *Physics Reports*, **222**, 145.

[6] Chen, H. (1995). *J. Stat. Phys.*, **81**, 347.

[7] Succi, S., Bella, G., Chen, H., Molvig, K. and Teixeira, C. (1998). *Proceedings of "Computer simulations of rare events and the dynamics of classical and quantum condensed phase systems"*, World Scientific Singapore, p. 269.

[8] Succi, S., Bella, G., Chen, H., Molvig, K. and Teixeira, C. (1999). *J. Comp. Phys.*, **152**, 493.

[9] Amdsen, A., O' Rourke, P. and Butler, T., *KIVA-II: a computer program for chemical reactive flows with sprays*, Los Alamos Report, 11560-RS, UC-96, May, 1989.

[10] Oran, E. and Boris, J., Numerical simulation of reactive flow, Elsevier Science, New York, 1987.

[11] Silverberg, M., Ben-Shaul, A. and Rebentrost, F. (1985). *J. Chem. Phys.*, **83**(12), 6501.

[12] Stampfl, C. and Scheffler, M. (1997). *Phys. Rev. Lett.*, **78**(8), 1500.

[13] Chen, D. K. S. and Cole, C. (1982). Society Automotive Engineers, paper 890798, 1989; Oh, S. and Cavendish, J., *Ind. Eng. Chem. Res. Develop.*, **21**, 29.